Nuclear Physics B101 (1975) 429–449

TOTAL AND INCLUSIVE e^+e^- ANNIHILATION "UNDERSTOOD" FROM A SCALING MODEL FOR DEEP INELASTIC ELECTRON SCATTERING

G. SCHIERHOLZ
CERN, Geneva

M.G. SCHMIDT*
Institut für Theoretische Physik, Heidelberg

Received 29 May 1975

It is shown that the seeming contradiction between deep inelastic electron scattering and e^+e^- annihilation can be resolved by taking proper account of anomalous singularities in the annihilation structure functions, corresponding to resonance mediated final states.

1. Introduction

The recent SPEAR data of hadron production in e^+e^- collisions [1] contradicted most ideas of photon-induced hadron production existing up to one year ago. Based on elementary quark-parton model ideas or naive analytical continuation of the deep inelastic electron scattering data, the inclusive annihilation cross section was expected to scale and the total cross section to behave "pointlike" (i.e., to be proportional to $1/q^2$). The SPEAR data, on the other hand, show that at present energies ($q^2 \lesssim 25$ GeV^2) scaling is badly violated at large x, i.e., at low momenta ($x = 1/\omega = -q^2/2m\nu$) and seems only to be valid in the small x region ($x \lesssim 2$). This results in a more or less constant total cross section** over the whole SPEAR energy range instead of an expected $1/q^2$ dependence.

Adding to all this confusion, two narrow resonances coupling to the e^+e^- channel have been found very recently [2] at a mass of 3.1 and 3.7 GeV, respectively. It is tempting to connect the physics of these resonances to the near constancy of the total cross section. But so far, we cannot see any answer to the question why scaling is badly violated at large x whereas it seems to be valid for large momenta. On the

* Address after May 1: CERN, Geneva.

** The latest edition of the SPEAR data though has discovered some oscillations superimposed on it.

contrary, suppose there is a threshold at 4.2 GeV associated with any new hadronic degree of freedom, then we would expect that scaling be violated in the small x region which apparently is not the case.

All our expectations towards hadron production in e^+e^- collisions were based on the assumption that the ideas borne out of the deep inelastic electron (and neutrino) scattering experiments can literally be taken over to the timelike region. The SPEAR results now reveal that the spacelike and timelike regions are unlikely to be connected in a simple manner, a fact which has long been advocated by several authors [3–6].

From an S-matrix point of view it seems indeed more natural that the deep inelastic scattering and annihilation structure functions are not connected via analytical continuation. A simple relationship is only accomplished for a very restricted set of Feynman diagrams [7]. Generally, the annihilation structure function receives contributions from anomalous singularities [3, 4] which move onto the physical sheet as the external masses are increased [8].

Before one now attributes the violation of scaling to some new phenomenon, and in order to see how far the e^+e^- cross section reflects the new physics behind the narrow resonances, one should (re-)examine what current scaling models really predict in the annihilation region taking account of the full analytical structure. This may reveal that the SPEAR results do not contradict asymptotic scaling and perhaps will clarify what the origin of the behaviour of the total cross section is.

Such an analysis requires, of course, a definite model. It is the aim of this paper to investigate how far the total and inclusive e^+e^- cross section can be understood from the recently proposed dual light cone model [9, 10].

The paper is organized as follows. In sect. 2, we give a brief review of the dual light cone model. In sect. 3 we discuss the analytical continuation into the timelike region in detail. Particular interest is devoted to anomalous singularities contributing to the annihilation structure functions. In sect. 4 (and sect. 3), it is argued that the anomalous singularity contributions can be saturated in a fairly neat way without introducing any new parameter. Quantitatively, it turns out that these contributions can indeed resolve most of the seeming contradiction between lepton induced hadron production at space and timelike q^2. Finally, in sect. 5 we add some concluding remarks.

2. The dual light cone model

The recently proposed dual light cone model [9] will be the main building block of our program sketched so far. Before we go into any details let us first briefly recapitulate the basic features of this model*.

In the deep inelastic scattering region the Compton amplitude could be written

* See also ref. [11].

$$A(s,t=0;q^2,q'^2) = -\int_0^1 \mathrm{d}\alpha \int_{-(1-\alpha)}^{1-\alpha} \mathrm{d}\beta \frac{F(\alpha,\beta)}{[\frac{1}{2}(q^2+q'^2)(1-\alpha)+\frac{1}{2}(q^2-q'^2)\beta + s\alpha]}, \tag{2.1}$$

where

$$F(\alpha,\beta) = N\alpha^{-\alpha(0)+1}\left(\frac{(1-\alpha)^2-\beta^2}{4}\right)^{c_1}\left(\frac{(1+\alpha)^2-\beta^2}{4}\right)^{-c_1+c_1'+\alpha(0)-2}, \tag{2.2}$$

which led to the deep inelastic structure function

$$F_2(x) = \int_{-(1-x)}^{1-x} \mathrm{d}\beta\, F(x,\beta) = N x^{-\alpha(0)+1}(1-x)^{2c_1+1} \times \int_{-1}^{+1} \mathrm{d}\beta' \left(\frac{1-\beta'^2}{4}\right)^{c_1}\left(\frac{(1+x)^2-(1-x)^2\beta'^2}{4}\right)^{-c_1+c_1'+\alpha(0)-2}. \tag{2.3}$$

The transverse structure function $F_1(x)$ was given by means of the Callan-Gross relation

$$F_1(x) = \frac{1}{2mx} F_2(x), \tag{2.4}$$

(m being the target mass) which we expect to hold, *irrespective* of the spin of the underlying constituents. The normalization of the light cone spectral function (i.e., N) was provided by the Adler sum rule [$\alpha(0) < 1$]

$$\int_0^1 \frac{\mathrm{d}x}{x} F_2(x) = 1, \tag{2.5}$$

which, being a consequence of the current algebra constraints, actually led to scaling.

Originally, eqs. (2.1)–(2.5) were derived for spin-zero targets. The generalization to higher-spin particles is not obvious*. In this paper we shall assume the spin-averaged structure functions to be the same as for spin-zero particles which, for the lowest-lying states, is supported by SU(6), SU(3) × SU(3), etc.

The deep inelastic structure functions are completely determined if the parameters c_1 and c_1' (corresponding to constant trajectories in the exotic quark hadron channels) are known. The parameter c_1 is related to the large q^2 behaviour of the spin-averaged (if any) target form factor, i.e.,

$$F(q^2) \simeq \frac{1}{(q^2)^{c_1+1}}, \tag{2.6}$$

* For a different choice abstracted from a dual eight-point function see [29].

in accordance with the Drell-Yan threshold relation [12] [cf. eq. (2.3)]. The parameter c_1' is determined by the asymptotic behaviour of the $(2^+) \to (1^-)$ transition form factors (e.g., $A_2 \to \rho\gamma$), i.e.,

$$F_{\text{trans}}(q^2) \simeq \frac{1}{(q^2)^{c_1'+1}} , \tag{2.7}$$

which results from going to the vector meson pole in the q'^2 channel and to the tensor meson pole in the t channel. For pions we take $c_1 = 0$ corresponding to a (commonly believed) monopole form factor [13]. The "scaling law" describing the asymptotic behaviour of the higher-spin form factors [14, 15] then predicts $c_1' = 2$ (independent of the target) which we will assume here. For nucleons we take $c_1 = 1$ corresponding to a dipole form factor [16]. Later on we are also interested in higher-spin structure functions which then may only differ in the threshold behaviour (i.e., c_1).

The dual light cone model includes normal threshold singularities only. Hence, we are not surprised that the deep inelastic annihilation structure functions are (for integer c_1, i.e., multipole behaviour of the target form factor which will be of interest only here) given by analytic continuation of the scattering structure functions (2.3) and (2.4). The somewhat confined analytic structure of the dual light cone model (Mandelstam analyticity) manifests itself also in the Gribov-Lipatov reciprocity relation [17] (holding quite generally for arbitrary c_1)

$$\begin{aligned} \bar{F}_2(x) &= x^3 F_2\left(\frac{1}{x}\right), \\ \bar{F}_1(x) &= x F_1\left(\frac{1}{x}\right), \end{aligned} \tag{2.8}$$

which relates $\bar{F}_1$, $\bar{F}_2$ and F_1, F_2 in their physical regions. Eq. (2.8) can easily be derived from eqs. (2.3) and (2.4).

The structure functions F_1, F_2 correspond to "charged" photon scattering. In order to obtain the physical structure functions, we have to perform an isospin rotation. Assuming SU(3), non-exoticity in all channels and the photon being a U spin scalar, we obtain

$$F_2^{\pi^\pm,\pi^0,K^\pm}(x) = \tfrac{5}{2}F_2^{K^0,\bar{K}^0}(x) = \tfrac{5}{4}F_2^{\eta 0}(x) = \tfrac{5}{3}F_2^{\eta 8}(x) = \tfrac{5}{9}F_2(x) \tag{2.9}$$

and similarly for any other meson nonet. In the case of the baryon octet, one has to allow for a $10(\overline{10})$ representation in the baryonic channels, and there is an infinite set of solutions to the requirements of SU(3) and non-exoticity. One (extreme) solution would be assuming that the decuplet does not contribute in the scaling region which would give the analogue of eq. (2.9). There is no doubt that the decuplet contributes to the scaling structure functions [18]. However, in the threshold region

(i.e., $x \approx 1$) this seems to be a good approximation. The $\Delta(1236) \to N$ transition form factor shows a faster decrease [19] than the nucleon form factor, which suggests a suppression of the decuplet contribution near $x = 1$ *via* the Drell-Yan relation. This solution predicts

$$\frac{F_2^n(x)}{F_2^p(x)}\underset{x\approx 1}{=}\frac{2}{5}, \tag{2.10}$$

being also supported by recent SLAC data [19]. Another (extreme) solution would be the SU(6)/quark model result

$$F_2^{p,\Sigma^+}(x) = \tfrac{3}{2}\,F_2^{n,\Sigma^0,\Xi^0,\Lambda} = 3F_2^{\Sigma^-,\Xi^-}(x) = F_2(x)\,, \tag{2.11}$$

which treats nucleon and Δ on the same footing. For small x, i.e., in the Regge region we consider this solution the most realistic one as it restores the characteristic features of the data here most adequately*. Later on we shall also be interested in the decuplet structure functions. Taking the SU(6)/quark model solution, they are given by

$$\tfrac{3}{4}F_2^{\Delta^{++}}(x) = F_2^{\Delta^+,Y^{*+}}(x) = \tfrac{3}{2}F_2^{\Delta^0,\Xi^{*0},Y^{*0}}(x) = 3F_2^{\Delta^-,\Xi^{*-},Y^{*-},\Omega^-}(x) = F_2(x)\,. \tag{2.12}$$

So far we have left out the pomeron contribution to the structure functions. This contribution cannot be integrated in the current algebra duality scheme, but has to be added by hand. Since our ansatz for the light cone spectral function can also be understood to provide a simple parametrization for the structure functions having Regge asymptotics and a definite threshold behaviour and satisfying the Gribov-Lipatov reciprocity relation (2.8), it is tempting to assume the same ansatz also for the diffractive part. In the context of our model this can also be motivated by assuming some s-channel background trajectory without resonances (remember, our model has non-linear trajectories) being dual to the pomeron in accordance with the Harari-Freund hypothesis. Now, the threshold behaviour (i.e., c_1) is, however, no longer determined by the asymptotic behaviour of any form factor. But, following the general belief that the background corresponds to (at least) two quark-antiquark pairs and three quarks, plus a quark-antiquark pair in the case of the pion and nucleon, respectively, we are tempted to set $c_1 = 2$ for pions and $c_1 = 3$ for nucleons according to the dimensional counting laws [22]. Hence, we expect the

* This will become evident by comparing the predictions of this model [fig. 1 and eq. (2.11)] to the neutron data [20, 21].

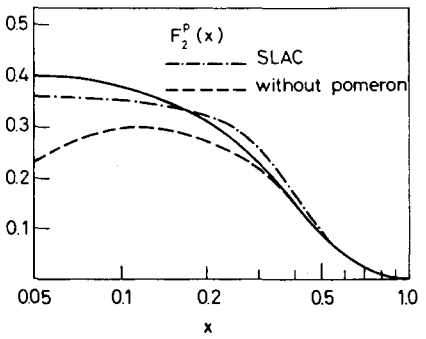

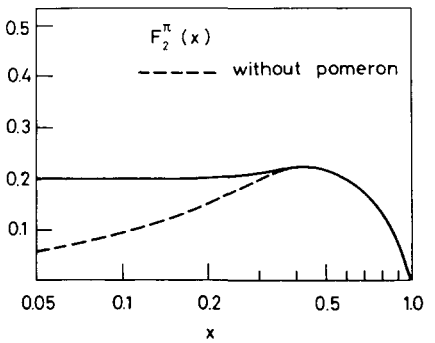

Fig. 1. The proton scaling function.

Fig. 2. The pion scaling function.

pomeron contribution to be strongly suppressed near threshold as compared to the non-diffractive part.

Let us now test our model at the deep inelastic scattering data. The intercept of the Regge trajectory [cf. eq. (2.3)] will be chosen $\alpha(0) = 0.3$ corresponding to a trajectory rising linearly up to the A_2 (or f) resonance with $\alpha'(0) = 1\ \mathrm{GeV}^{-2}$. Then the pomeron coupling remains the only free parameter. We assume the pomeron being a SU(3) singlet. Choosing the SU(6)/ quark model solution (for the nucleon octet), we obtain a good fit to the proton data for $N_{\mathrm{pomeron}} = 2$ as shown in fig. 1. Also indicated is the non-diffractive part of the proton structure function (which contains no free parameter). This, by itself, is also in good agreement with recent neutrino experiments [23] which we consider, giving strong support to our ideas. The pomeron contribution is significant at small x only as we expected being consistent with the data.

In the meson case the pomeron coupling is now determined via factorization by the (experimental) ratio $\sigma_{\mathrm{tot}}^{\pi p}/\sigma_{\mathrm{tot}}^{pp} \approx \frac{2}{3}$ (note that the $x \to 0$ limit of the scaling structure functions does not depend on c_1) or, giving the same result, assuming additivity of the quark pomeron couplings. The resulting structure function is shown in fig. 2. Due to the different threshold factor, $F_2^\pi(x)$ increases much faster near threshold than the proton structure function. The pomeron contribution again is negligible for large x.

The scaling structure functions are meaningless as they stand if scaling is reached asymptotically only. To the next leading order the Compton amplitude A is given by [neglecting curvature of the Regge trajectories; cf. ref. [9], following eq. (4.10)]

$$A(s,t=0;q^2,q'^2) = -\int_0^1 \mathrm{d}\alpha \int_{-(1-\alpha)}^{1-\alpha} \mathrm{d}\beta \times \frac{F(\alpha,\beta)}{\frac{1}{2}(q^2+q'^2)(1-\alpha)+\frac{1}{2}(q^2-q'^2)\beta + s\alpha + \frac{\frac{1}{2}+c_1-\alpha(0)}{\alpha'(0)}\alpha + \frac{\frac{1}{2}+\alpha(0)}{\alpha'(0)}}, \quad (2.13)$$

which results in the structure function

$$F_2(x, q^2) = \int_{-(1-x')}^{1-x'} d\beta\, F(x', \beta) \left[1 - \frac{x}{\alpha'(0)q^2}(\tfrac{1}{2} + c_1 - \alpha(0))\right]^{-1}$$

$$= F_2(x') \left[1 - \frac{x}{\alpha'(0)q^2}(\tfrac{1}{2} + c_1 - \alpha(0)\right]^{-1}, \tag{2.14}$$

where

$$x' = x \frac{1 + \frac{1}{\alpha'(0)q^2}(\frac{1}{2} + \alpha(0))}{1 - \frac{x}{\alpha'(0)q^2}(\frac{1}{2} + c_1 - \alpha(0))}. \tag{2.15}$$

Here, $\alpha(0)$ means the intercept of the trajectory in the photon channel. The variable x' has long been advocated by Bloom and Gilman [18] and by Rittenberg and Rubinstein [24,25].

3. Continuation to the timelike region

Once again, we emphasize that the dual light cone model has only normal threshold singularities which led to the simple reciprocity relation (2.8) connecting the timelike and spacelike region. In general, the continuation to timelike q^2 reads

$$\mathrm{disc}_s \frac{\nu}{\pi} A(s, 0; q^2 + i\epsilon, q^2 - i\epsilon) = -\,\mathrm{Re}\,\mathrm{disc}_s \frac{\nu}{\pi} A(s, 0; q^2 + i\epsilon, q^2 + i\epsilon) + G(s, q^2), \tag{3.1}$$

where $G(s,q^2)$ is the triple discontinuity* [26] (in s, q^2, q'^2). So far $G(s,q^2)$, as given by the dual light cone model, was zero for the cases we were interested in. We had [9]

$$G(x) = 2N \sin^2 \pi c_1\, x^{-\alpha(0)+1}(x-1)^{2c_1+1}$$

$$\times \int_{-1}^{+1} d\beta' \left(\frac{1-\beta'^2}{4}\right)^{c_1} \left(\frac{(1+x)^2 - (1-x)^2\beta'^2}{4}\right)^{-c_1+c_1'+\alpha(0)-2}, \tag{3.2}$$

which vanishes for integer c_1.

The Gribov-Lipatov relation is now valid for any c_1, i.e., $G \neq 0$ even. Hence, the triple discontinuity contribution arising from normal threshold singularities [26] [eq. (3.2)] is properly considered by simply employing the reciprocity relation (2.8) in continuing to the timelike region.

* Strictly speaking, in the definition of eq. (3.1) this is only true for nucleons.

The triple discontinuity G also receives, however, contributions from anomalous singularities [3] moving onto the physical sheet as the external masses are increased [8]. Typical examples are graphs with unstable external (the photon) and internal particles as have extensively been discussed by Gatto, Menotti and Vendramin [4]. These contributions are expected to violate the Gribov-Lipatov relation and will have to be treated separately. The derivation of the reciprocity relation given by one of us [27], being based on S matrix theory, substantially relied upon the assumption of a Mandelstam representation for the Compton amplitude for spacelike and timelike q^2. If anomalous singularities now become important in the timelike region the Mandelstam representation will necessarily break down here. It will, however, continue to hold for spacelike q^2.

The generalized box graph as shown in fig. 3 is the first graph to acquire anomalous singularities as the external masses are increased [8] and also survives in the scaling limit. Here the horizontal lines may be any resonance having a non-vanishing deep inelastic structure function. Any other line inserted into this graph delays the onset of these anomalous singularities. Hence, the generalized box graph enclosing the well-established (boson and fermion) resonances seems to be a fairly well approximation of the anomalous singularity contributions.

The triple discontinuity G, i.e., the "bare" anomalous singularity contribution of the box graph (fig. 3) corresponds to the resonance mediated final state as shown in fig. 4, where the resonance is on its mass shell [4]. It is obvious that adding these contributions to the analytically continued normal threshold part does not cause any kind of double counting. The normal threshold part of the box graph, however, is generally being taken care of by Re $\mathrm{disc}_s A(s, 0; q^2 + i\epsilon, q^2 + i\epsilon)$ or, in particular, by the Gribov-Lipatov relation. We will come back to this question at the end of this section.

Let us now concentrate on the "bare" anomalous singularity contributions to the deep inelastic (annihilation) structure functions. For the moment we shall consider a single resonance only (cf. fig. 4) and assume that all spin states (of the resonances, if any) are produced with equal strength. We also assume that the deep in-

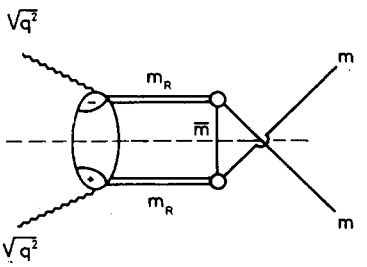

Fig. 3. Generalized box diagram giving rise to anomalous singularities for $m_R^2 > \bar{m}^2 + m^2$.

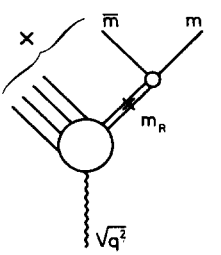

Fig. 4. The bare anomalous singularity contribution of the box diagram. The resonance R is on its mass shell.

elastic resonance structure function describing the lower vertex in fig. 4 contains no (further) anomalous singularities. The case of double box graphs (with three rungs) going beyond this assumption will be discussed later on.

Since we are dealing with two structure functions we now write

$$\bar{F}_1(x) = \mathrm{Re}\, F_1(x) + G_1(s, q^2)\,,$$

$$\bar{F}_2(x) = -\mathrm{Re}\, F_2(x) + G_2(s, q^2)\,. \tag{3.3}$$

In the zero-width limit we then have

$$2mG_1 - \frac{\beta^2}{2x} G_2 \sin^2\theta = \frac{m_R}{\pi p_R^{cm}} (2J_R + 1) \int \frac{d^3p_R}{2p_{0R}} \int \frac{d^3p}{2\bar{p}_0}$$

$$\times\, \delta^{(4)}(p_R - \bar{p} - p) \left(2m_R \bar{F}_1^R(x_R) - \frac{\beta_R^2}{2x_R} \bar{F}_2^R(x_R) \sin^2\theta_R\right), \tag{3.4}$$

where $m(m_R)$ is the mass of the detected hadron (resonance), $\theta(\theta_R)$ its angle relative to the beam axis, $\beta^2 = 1 - 4m^2x^2/q^2$, $x_R = \sqrt{q^2}/2p_{0R}$ and $\beta_R^2 = 1 - 4m_R^2x_R^2/q^2$. Furthermore $p_R^{cm} = \sqrt{(m_R^2 - (\bar{m} + m)^2)(m_R^2 - (\bar{m} - m)^2)}/2m_R$ where $\bar{m}$ is the mass of the secondary decay product of the resonance R. The resonance structure functions are understood spin averaged (spin J_R) which gives rise to the multiplicity factor $2J_R + 1$. In the case where secondary and detected particle are equal, the right-hand side of eq. (3.4) has to be multiplied by an additional factor of two.

The phase space integral in eq. (3.4) can be written in terms of an integral over x_R and $\cos\theta_R$ giving

$$2mG_1 - \frac{\beta^2}{2x} G_2 \sin^2\theta = \frac{2m_R}{\pi p_R^{cm}} (2J_R + 1)$$

$$\times \int_{D<0} dx_R\, d\cos\theta_R\, \frac{\beta_R}{16x_R^3\sqrt{-D}} (2m_R \bar{F}_1^R(x_R) - \frac{\beta_R^2}{2x_R} \bar{F}_2^R(x_R) \sin^2\theta_R)\,, \tag{3.5}$$

where

$$D = \left[\frac{\beta}{4xx_R}(\beta\cos\theta - \beta_R\cos\theta_R) + \frac{\cos\theta}{q^2}\left(m^2\frac{x}{x_R} - \tfrac{1}{2}(m_R^2 + m^2 - \bar{m}^2)\right)\right]^2$$

$$+ \frac{\sin^2\theta}{q^2}\left[\frac{1}{4}\left(\frac{m^2}{x_R^2} - \frac{(m_R^2 + m^2 - \bar{m}^2)}{xx_R} + \frac{m_R^2}{x^2}\right) - \frac{1}{q^2}(m^2m_R^2 - \tfrac{1}{4}(m_R^2 + m^2 - \bar{m}^2)^2)\right]. \tag{3.6}$$

The integral over $\cos\theta_R$ can now be carried out analytically. Substituting $x_R = x/\eta$ this finally gives

$$2mG_1 = \frac{m_R}{2p_R^{cm}}(2J_R+1)\frac{1}{\beta}\int_{\eta_1}^{\min(x,\eta_2)} d\eta\,(2m_R\,\bar{F}_1^R(x/\eta)$$

$$-\left[\beta_R^2-\beta^2\left(1+\frac{4x^2}{\beta^2q^2\eta}(m^2\eta-\tfrac{1}{4}(m_R^2+m^2-\bar{m}^2)\right)^2\right]\frac{\eta}{2x}\,\bar{F}_2^R(x/\eta))\,, \quad (3.7)$$

$$\frac{\beta^2}{2x}G_2 = \frac{m_R}{2p_R^{cm}}(2J_R+1)\frac{1}{\beta}\int_{\eta_1}^{\min(x,\eta_2)} d\eta\left[\beta^2\left(1+\frac{4x^2}{\beta^2q^2\eta}(m^2\eta-\tfrac{1}{4}(m_R^2+m^2\right.\right.$$

$$\left.-\bar{m}^2)\right)^2+\frac{8x^4}{\beta^2q^2\eta^2}\left(\frac{1}{4x^2}(m^2\eta^2-(m_R^2+m^2-\bar{m}^2)\eta+m_R^2)\right.$$

$$\left.\left.+\frac{1}{q^2}(m^2m_R^2-\tfrac{1}{4}(m_R^2+m^2-\bar{m}^2)^2)\right)\right]\frac{\eta}{2x}\bar{F}_2^R(x/\eta)\,, \quad (3.8)$$

where

$$\eta_{1,2} = \frac{m_R^2+m^2-\bar{m}^2}{2m^2} \mp \left(\left(\frac{m_R^2+m^2-\bar{m}^2}{2m^2}\right)^2-\frac{m_R^2}{m^2}\right.$$

$$\left.+\frac{4x^2}{m^2q^2}(m^2m_R^2-\tfrac{1}{4}(m_R^2+m^2-\bar{m}^2)^2)\right)^{1/2}. \quad (3.9)$$

Asymptotically, i.e., as $q^2 \to +\infty$ eqs. (3.7) and (3.8) reduce to

$$2mG_1 = \frac{m_R}{2p_R^{cm}}(2J_R+1)\int_{\eta_1^\infty}^{\min(x,\eta_2^\infty)} d\eta\,2m_R\,\bar{F}_1^R(x/\eta)\,, \quad (3.10)$$

$$\frac{1}{2x}G_2 = \frac{m_R}{2p_R^{cm}}(2J_R+1)\int_{\eta_1^\infty}^{\min(x,\eta_2^\infty)} d\eta\,\frac{\eta}{2x}\,\bar{F}_2^R(x/\eta)\,, \quad (3.11)$$

respectively.

The anomalous singularity contributions scale non-trivially as we expected. The approach to scaling is, however, substantially retarded especially at large x as compared to the normal threshold contribution. If the (normal threshold) resonance scaling functions fullfil the Callan-Gross relation this is asymptotically also retained in the anomalous singularity contributions [cf. eqs. (3.10) and (3.11)]. For finite q^2 the Callan-Gross relation gets, however, strongly modified.

Since our model incorporates Mandelstam analyticity, the normal threshold part of the box diagram (fig. 3) is already included in the structure functions (2.3), (2.4)

and (2.8) so that the complete annihilation structure functions are given by eq. (2.8) plus the anomalous singularity contributions [eqs. (3.7) and (3.8)].

4. Predictions for timelike q^2

In the last section we have strongly exposed the anomalous singularity contributions to the e^+e^- annihilation structure functions. Before we go into any detailed numerical discussion, let us now ask how large we expect the anomalous singularity contributions to be, compared to the analytically continued normal threshold part. In figs. 5 and 6 we have drawn the (normal threshold) antiproton and pion annihilation structure functions $\bar{F}_2^{\bar{p}}(x)$ and $\bar{F}_2^{\pi}(x)$, respectively, as given by the reciprocity relation (2.8), compared to the SPEAR data [28]. We find that the normal threshold (anti-)proton structure function roughly accounts for the data. Note also that the experimental antiproton distribution seems to depend far less on q^2 than in the case of the pion (cf. fig. 6). This means (in our language) that, at present energies, the anomalous singularity contributions to the (anti-)proton structure functions should not be sizeable. In the case of the pion distribution, we are, however, confronted with a rather different situation. Here (cf. fig. 6), the analytically continued normal threshold part is substantially below the experiment and does in no way follow the trend of the data, i.e., the seeming violation of scaling at large x (small ω). The discrepancy is most striking in the large x region and decreases as x is decreasing. This leads us to conclude that in the case of the pion distribution, the anomalous singularity contributions have to account for most of the data and for the violation of scaling, *exhibiting a second, x-dependent scale.*

Can the anomalous singularity contributions as discussed in sect. 3 now describe these features of the deep inelastic annihilation data? The answer is yes, as we shall see later on in this section.

The magnitude of the anomalous singularity contributions (cf. sect. 3) depends on the masses of the resonance and its decay products and on the nature of the structure functions $\bar{F}_{1,2}^{R}(x)$. Moreover, it depends on the multiplicity of the inclusive (say) pion in the final state of the resonance R including the spin factor $2J_R + 1$.

As far as the x-dependence is concerned, we expect the anomalous singularity contributions at present q^2 ($q^2 \lesssim 25$ GeV^2) to be zero for $x \lesssim 1.2 - 1.6$, depending on the kinematical configuration, due to the fact that the lower limit of the integral in eqs. (3.7) and (3.8) exceeds its upper limit in this region. At large x, however, both the anomalous singularity and normal threshold contributions have the same power behaviour (remember, $c_1' = 2$ holds irrespective of the nature of the target/inclusive particle). Hence, the anomalous singularity contributions are expected to lead to an enhancement of the analytically continued inclusive distribution at large x (provided both are at least of the same order of magnitude) whereas at small x they die away rapidly. This is exactly how the extra contributions missed out in the analytic continuation should look like (cf. fig. 5).

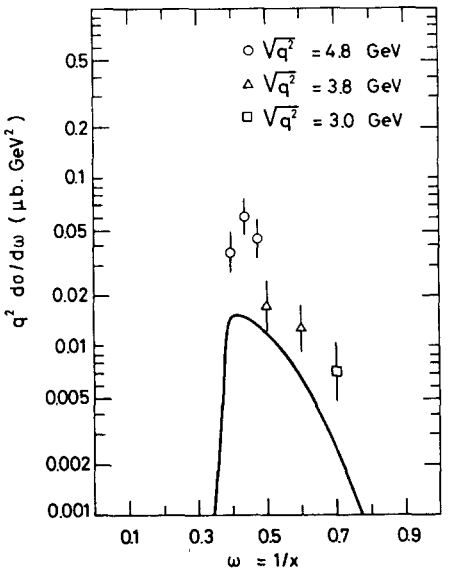

Fig. 5. The antiproton distribution as given by the Gribov-Lipatov reciprocity relation compared to the SPEAR data.

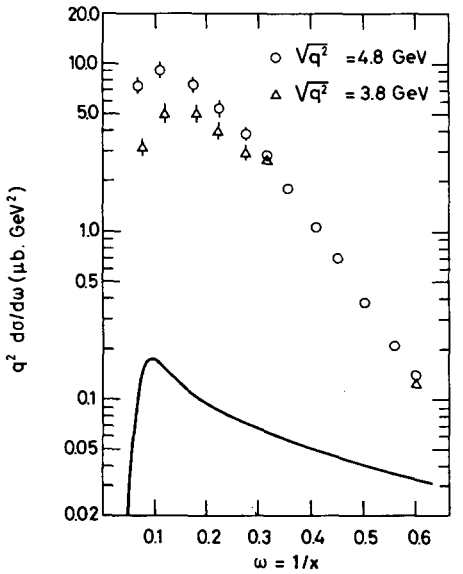

Fig. 6. The pion distribution as given by the Gribov-Lipatov reciprocity relation in our model (i.e., the normal threshold part) compared to the SPEAR data.

For small and medium x the η integration [cf. eqs. (3.7) and (3.8)] extends over the threshold region of $\bar{F}^{R}_{1,2}(x/\eta)$, so that the magnitude of the anomalous singularity contributions strongly depends on the actual threshold behaviour of $\bar{F}^{R}_{1,2}(x)$ in this

domain. From general arguments given later on in this section, we conclude that the low-lying meson (baryon) resonances such as, e.g., the $\rho(\Delta(1236))$ should give rise to the same threshold behaviour as the pion (proton) structure function, i.e., $\bar{F}_{1,2}(x) \simeq x - 1$ ($\bar{F}_{1,2}(x) \simeq (x-1)^3$). Because of the higher threshold factor inherent in the nucleon scaling functions, we then expect that the anomalous singularity contributions to the nucleon inclusive distribution (e.g., $R = \Delta \to N\pi$) are much smaller than those arising from the meson resonances (e.g., $R = \rho \to 2\pi$) and contributing to the pion spectrum. For the same reason the contribution of the baryon resonances to the pion inclusive distribution and any other contribution accompanied with a higher threshold factor should be relatively small too for small and medium x.

This symptom of the anomalous singularity contributions can also be traced in the SPEAR data. At present energies, the (anti-)proton inclusive distribution is roughly described by the normal threshold part (cf. fig. 5; note that the nucleon inclusive distribution is for $q^2 \lesssim 25$ GeV^2 constrained to small and medium x, i.e., $x \lesssim 2.8$), whereas the experimental pion inclusive cross section is substantially larger than the (predicted, though well founded) normal threshold contribution even at medium x (cf. fig. 6).

For large x (and fixed q^2) the small η region of integration [cf. eqs. (3.7) and (3.8)] is sensitively cut-off by the lower limit η_1. At $x = 10$ and $q^2 = 25$ GeV^2 we find for various (representative) cases (the detected particle being underlined)

R	η_1
$\rho \to 2\pi$	3.75
f $\to 2\pi$	8.25
$A_1 \to \underline{\pi}\rho$	4.51
$A_2 \to \underline{\pi}\rho$	6.38
$\Delta \to \underline{\pi}N$	4.96

(4.1)

Hence, even here the η integration is confined to the threshold region of $\bar{F}^R_{1,2}(x/\eta)$, so that the same argument, which let us expect any resonance contribution accompanied with a higher threshold factor being suppressed, also applies in this region. Moreover, as η_1 increases with m_R^2 [cf. table (4.1)], we conclude that higher mass resonances are as well strongly suppressed for any threshold behaviour (note that the large x region provides by far the dominant contribution to the cross section). For finite q^2 this leaves us with a rather comprehensible situation of saturating the anomalous singularity contributions by the well-established low-lying resonances.

Asymptotically, the η integration is, however, no longer confined to the threshold region and the higher mass resonances are not suppressed anymore so that there is a priori no reason why anomalous singularity contributions involving higher threshold factors and/or higher mass resonances should not become significant here.

We notice that the anomalous singularity contributions involve a new scale being typically of the other $4m_R^2x^2/\langle\eta\rangle^2$, where $\langle\eta\rangle$ can be defined by

$$\langle\eta\rangle \approx \left[\int_{\eta_1}^{\min(x,\eta_2^\infty)} d\eta\, \bar{F}_2^R\left(\frac{x}{\eta}\right)\right]^{-1} \int_{\eta_1}^{\min(x,\eta_2^\infty)} d\eta\, \eta\, \bar{F}_2^R\left(\frac{x}{\eta}\right). \tag{4.2}$$

For $R = \rho \to 2\pi$ and $c_1 = 0$ [i.e., $\bar{F}_{1,2}^{\rho}(x) \simeq x - 1$ as $x \to 1$], which provides a substantial contribution to the inclusive pion distribution as we shall see, we obtain $\langle\eta\rangle \approx 2$ introducing a scale of about $m_\rho^2 x^2$ for this particular contribution (this is not to be confused with η_1 being given for finite q^2). Hence, for any q^2 there will be a region of large x (shrinking to zero as q^2 is increasing) where scaling has not yet been reached. This means that we cannot expect scaling at large x (its lower limit depending on q^2) whereas we do expect scaling for medium x and near threshold. For $R = \Delta \to N\pi$ and the nucleon being detected we obtain a scale of the same order of magnitude which certainly will show up in the nucleon distribution at large x. This region will become accessible at very high q^2, where our threshold argument clearly does not apply anymore.

Asymptotically, the angular distribution of the anomalous singularity contributions is $\sim(1 + \cos^2\theta)$ (cf. sect. 3). For finite q^2 this behaviour is, however, strongly influenced by the pre-asymptotic corrections occurring under the integral of eqs.

Table 1
Resonances taken into account in the anomalous singularity contributions

$q\bar{q}$ state	$I^G(J^P)$	R	Comments	Ideal decay modes
	$1^+(1^-)$	$\rho(770)$		2π
$^3S_1$	$\frac{1}{2}(1^-)$	K*(892)		$K\pi$
	$0^-(1^-)$	$\omega(784)$, $\varphi(1020)$	ideal mixing	3π, $K\bar{K}$
	$1^-(0^+)$	$\delta(920)$		$\pi\eta$
$^3P_0$	$\frac{1}{2}(0^+)$	$\kappa(1300)$		$K\pi$
	$0^+(0^+)$	$\epsilon(750)$, S*(1060)	ideal mixing	2π, $K\bar{K}$
	$1^-(1^+)$	$A_1(1100)$		$\pi\rho$
$^3P_1$	$\frac{1}{2}(1^+)$	$K_A(1300)$		$K\pi\pi$
	$0^+(1^+)$	D(1290), E(1420)	ideal mixing	$\pi\delta$, $K\bar{K}^* + \bar{K}K^*$
	$1^-(2^+)$	$A_2(1310)$		$\pi\rho$ (75%), $\pi\eta$(25%)
$^3P_2$	$\frac{1}{2}(2^+)$	$K_N(1420)$		$K\pi$ (60%), $K\pi\pi$ (40%)
	$0^+(2^+)$	f(1270), f'(1520)	ideal mixing	2π, $K\bar{K}$
	$1^+(1^+)$	B(1235)		$\pi\omega$
$^1P_1$	$\frac{1}{2}(1^+)$	$K_A(1300)$		$K\pi\pi$
	$0^-(1^+)$	?		

(3.7) and (3.8). Due to destructive interference between the leading and pre-asymptotic expressions, G_2 gets sensibly suppressed, especially at small q^2 and large x, which results in a more or less flattened angular distribution.

We have argued that the anomalous singularity contributions are for present values of q^2 well approximated by the low-lying resonances and those having the least suppressing threshold behaviour. In the context of our model, starting from non-linear trajectories, we now expect quite generally (i.e., for all q^2) that the anomalous singularity contributions can be saturated by a finite set of resonances. In the following we shall restrict ourselves to the decuplet, i.e., R = $\{\Delta, \Xi^*, Y^*, \Omega^-\}$ in the case of the baryons and to the meson resonances as listed in table 1. We believe this to be a good approximation even at very large q^2.

It is clear that the resonance structure functions entering in the anomalous singularity contributions should contain no anomalous singularities anymore (as, e.g., the ρ structure function would contain anomalous singularities if, e.g., the $A_1 \to \rho\pi$ intermediate states had not been included explicitly though it turned out to be important) if these are saturated by the given resonances. It is also clear that adding the various resonance terms does not cause any double counting as long as the resonance structure functions do not contain anomalous singularities. The double box graph corresponding to, e.g., the $A_1 \to \rho\pi$ decay chain (fig. 7a) can, as far as the anomalous singularity content is concerned, be rewritten in the form drawn in fig. 7b, so that these contributions are also covered by our general formalism (cf. sect. 3).

We now assume that the pomeron couples universally to all mesons and all baryons. Furthermore (for lack of any other information) we assume that the resonance form factors obey the "scaling law" being established by several authors [14, 15]. This means that the spin-averaged form factors

$$F(q^2) = (p_0 + p_0')^{-1} \left(\sum_{\lambda\lambda'} |\langle p\lambda | j_0(0) | p'\lambda' \rangle|^2 \right)^{1/2}$$

have a universal asymptotic behaviour of the form $\simeq (q^2)^{-1}$ and $\simeq (q^2)^{-2}$ for all meson and baryon resonances, respectively [cf. sect. 2 following eq. (2.7)]. Consequently, we set $c_1 = 0$ for meson targets and $c_1 = 1$ for baryons, which then com-

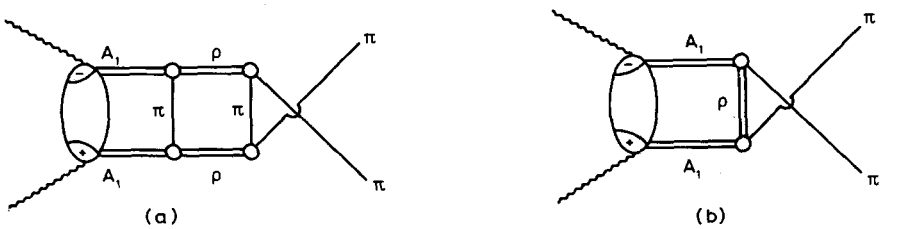

Fig. 7. Higher order anomalous singularity contributions. (a) and (b) give the same anomalous singularity contribution to the pion structure function.

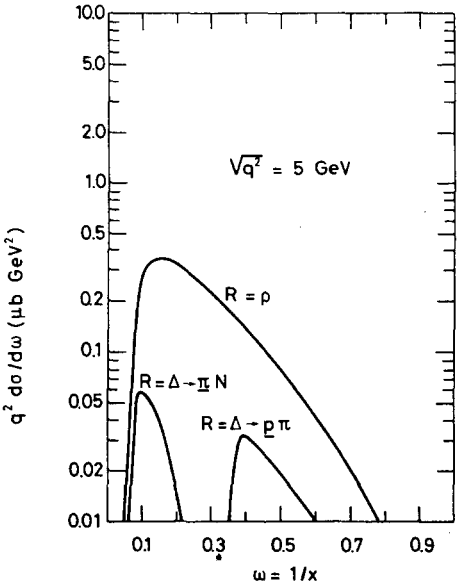

Fig. 8. Some typical anomalous singularity contributions. The detected particle is underlined.

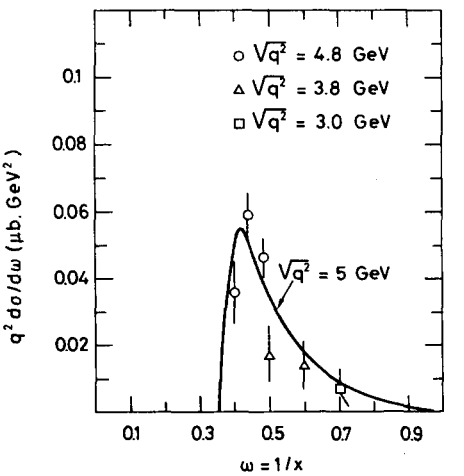

Fig. 9. The antiproton distribution including the Δ mediated anomalous singularity contribution compared to the SPEAR data.

pletely determines our input. The same results also follow from SU(6) at least for the lowest-lying resonances.

In the last part of this section we shall now discuss the predictions of our model stated so far for the total and inclusive e^+e^- annihilation cross section.

The differential cross section for $e^+e^- \to h + X$ has the form

$$q^2 \frac{d^2\sigma^h}{d\omega\, d\cos\theta} = \frac{\pi\alpha^2}{2x} \beta_h (2J_h + 1) \left[2m_h \bar{F}_1^h(x) - \frac{\beta_h^2}{2x} \bar{F}_2^h(x) \sin^2\theta \right], \quad (4.3)$$

where $\bar{F}_1^h$ and $\bar{F}_2^h$ are the (complete) annihilation structure functions as discussed in sect. 2 and $\omega = 1/x = 2E_h/\sqrt{q^2}$. Integrating out the angular dependence, this can be rewritten as

$$q^2 \frac{d\sigma^h}{d\omega} = \frac{\pi\alpha^2}{x} \beta_h (2J_h + 1) \left[2m_h \bar{F}_1^h(x) - \frac{2\beta_h^2}{3x} \bar{F}_2^h(x) \right]. \quad (4.4)$$

As a first numerical illustration of what we have aimed at in the beginning of this section, we have calculated the inclusive cross section for various anomalous singularity contributions (fig. 8). We see that, in fact, the Δ contributes much less than the ρ though the Δ has a higher multiplicity. We also notice that the shape of the anomalous singularity contributions is much different from that of the analytically continued distribution (cf. figs. 6 and 8), whereas it qualitatively follows the course of the data.

Let us now turn to the quantitative predictions. In fig. 9 we have drawn the (anti-)proton inclusive cross section as predicted by our model (i.e., including the anomalous singularity contribution arising from the Δ) together with the SPEAR data. The agreement is surprisingly good and may be considered as a first positive test of our ideas.

In case of the pion and kaon inclusive cross section there are many more terms to compute (cf. table 1). The result for charged pions plus kaons is shown in fig. 10. Here, the SPEAR data are well reproduced up to $\bar{\omega} \approx 0.2$. $[\bar{\omega} = (\omega^2 - [4m_h^2/q^2])^{1/2}]$ whereas for $\bar{\omega} < 0.2$, i.e., at the peak of the cross section the experimental distribution is somewhat higher (about 25%). Note, however, that the actual SPEAR data are likely to be *down by* $\approx$ *10% in this region,* since it has been assumed that all particles have pion mass in converting the measured inclusive cross section to $d\sigma/d\omega$.

We find this result very instructive. It states that the bulk of the inclusive cross section is due to anomalous singularity contributions. Moreover, it reveals that the SPEAR data do not contradict asymptotic scaling, contrary to many augurs. The x-dependent scale inherent in the anomalous singularity contributions accounts fairly well for the approach to scaling and, in particular, gives a plausible explanation why scaling is good at small x (large ω) but badly violated (at present energies) at low momenta. In fig. 10 we have also drawn our prediction for $\sqrt{q^2} = 10$ GeV. This shows that even the highest SPEAR energy ($\sqrt{q^2} = 5$ GeV) is still far away from asymptopia.

Fig. 11 shows the charged kaon inclusive cross section separately. At low momenta our calculations yield that kaons and pions are produced, independent of $q^2 (q^2 \leqslant 100\ \text{GeV}^2)$, in the ratio $K^c/\pi^c \approx 0.11$. For larger momenta this ratio increase substantially. At $x = 2$ we obtain $K^c/\pi^c \approx 0.25$ while $K^c/\pi^c = 1$ near threshold. This feature is also consistent with the SPEAR data.

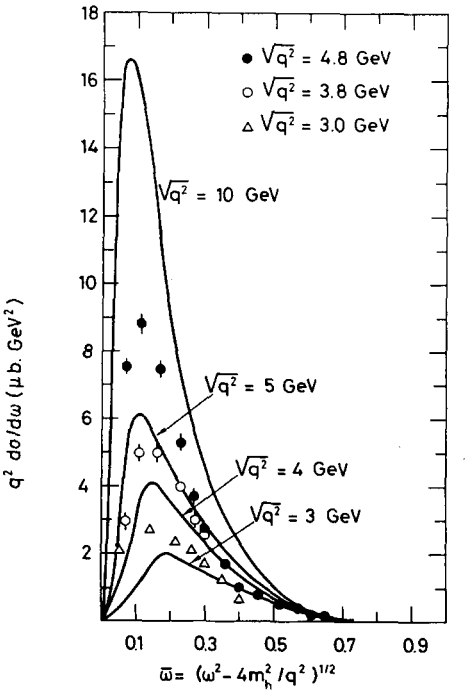

Fig. 10. Predicted (charged) inclusive cross section compared to the SPEAR data.

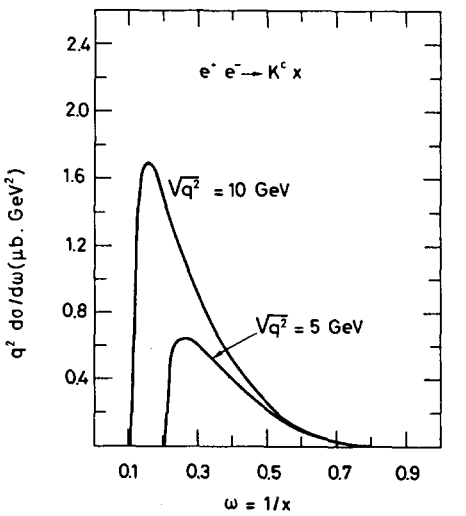

Fig. 11. Predicted (charged) kaon inclusive cross section.

The angular distribution can be parametrized in the form

$$\int_0^{0.5} d\omega \frac{d^2\sigma}{d\omega\, d\cos\theta} \sim 1 + \epsilon_1 \cos^2\theta ,$$

$$\int_{0.5}^{1} d\omega \frac{d^2\sigma}{d\omega\, d\cos\theta} \sim 1 + \epsilon_2 \cos^2\theta . \tag{4.5}$$

For various q^2 we obtain in our model

$\sqrt{q^2}$ (GeV)	ϵ_1	ϵ_2
3	0.08	0.2
4	0.1	0.35
5	0.15	0.45
10	0.3	0.85

(4.6)

This means that the over-all angular distribution looks rather flat since the small ω (large x) region accounts for most of the cross section. As far as ϵ_1 is concerned, our results agree nicely with the SPEAR data. In the scaling region ($\omega \geqslant 0.5$) the statistics are apparently too low to draw any conclusions. We expect ϵ_2 to go much faster to one than ϵ_1 which is not ruled out be experiment.

The total cross section is given by the energy sum rule

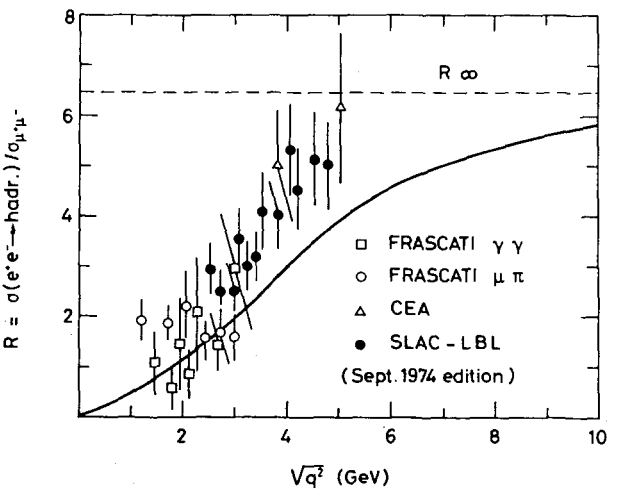

Fig. 12. Predicted total cross section compared to the world's data. The dotted line corresponds to the asymptotical cross section as predicted by our model.

$$\sigma(e^+e^- \to \text{hadrons}) = \frac{1}{2} \sum_h \int_{2m_h/\sqrt{q^2}}^1 d\omega\, \omega \frac{d\sigma^h}{d\omega}, \tag{4.7}$$

where the sum runs over all stable hadrons (i.e., the pion nonet and nucleon octet). The result of our calculation is shown in fig. 12 together with the world's data. The dotted line corresponds to the asymptotic value of the total cross section assuming that the anomalous singularity contributions are saturated by the decuplet and the resonances listed in table 1. We see that the asymptotic cross-section is attained very slowly. For small q^2 it joins nicely into the Frascati region, whereas at $q^2 = 25$ GeV^2 it stays $\approx 20\%$ below the SPEAR data.

Asymptotically, the ratio ρ_E = (charged energy)/(total energy) comes out to be* $\rho_E^\infty = \frac{5}{9}$ if only mesons are produced (cf. sect. 3). Numerically, ρ_E^∞ is reached already at SPEAR energies. This is in good agreement with the SPEAR data which tend to the value $\rho_E \approx 0.5$. If nucleons are also included, ρ_E^∞ gets slightly changed. Note, however, that the nucleon contribution can be neglected at SPEAR energies. Hence, there is no energy crisis in this model.

5. Conclusions

We have seen that the gross features of the SPEAR data can be understood by taking account of anomalous singularity contributions in the annihilation structure functions. The new resonances and the physics connected to it seem only to superimpose a fine structure on the total cross section.

At present q^2, the anomalous singularity contributions raise a fairly comprehensible situation. Here, only the low-lying resonances contribute which does not leave much freedom for numerical speculations. At very high q^2, however, it is not ruled out that higher resonances give a sensible contribution, meaning that the total cross section may well exceed R_∞ (cf. fig. 12) as predicted by our model.

Since the anomalous singularity contributions account for the bulk of the pion inclusive cross section, we expect this for the most part to be resonance mediated (cf. fig. 4), which should also show up in the e^+e^- data. It is now up to the experimentalists to provide the necessary data (e.g., the resonance structure functions) so as to clear up the situation further.

We wish to thank D. Amati for reading the manuscript.

References

[1] B. Richter, Proc. 17th Int. Conf. on high-energy physics, ed. J.R. Smith, (Science Research Council, Chilton, Didcot, 1974) p. IV-37.

* This does not contradict our earlier statements [10] where we had not included SU(3) singlets.

[2] J.J. Aubert et al., Phys. Rev. Letters 33 (1974) 1404;
J.E. Augustin et al., Phys. Rev. Letters 33 (1974) 1406;
C. Bacci et al., Phys. Rev. Letters 33 (1974) 1408, 1649 (erratum).
G.S. Abrams et al., Phys. Rev. Letters 33 (1974) 1453.
[3] A. Suri, Phys. Rev. D4 (1971) 510.
[4] R. Gatto, P. Menotti and I. Vendramin, Nuovo Cimento Letters 4 (1972) 79; Ann. of Phys. 79 (1973) 1.
[5] R. Gatto and G. Preparata, Nucl. Phys. B47 (1972) 313 (erratum B73 (1974) 548);
G. Schierholz and M.G. Schmidt, Phys. Letters 48B (1974) 341.
[6] P.V. Landshoff and J.C. Polkinghorne, Phys. Rev. D6 (1972) 3708.
[7] S.D. Drell, D.J. Levy and T.-M. Yan, Phys. Rev. 187 (1969) 2159; Phys. Rev. D1 (1970) 1617.
[8] R.J. Eden, P.V. Landshoff, D.I. Olive and J.C. Polkinghorne, The analytic S-Matrix (Cambridge University Press, New York, 1966).
[9] G. Schierholz and M.G. Schmidt, Phys. Rev. D10 (1974) 175.
[10] G. Schierholz and M.G. Schmidt, Phys. Letters 52B (1974) 467.
[11] D. Amati, S.D. Ellis and J.H. Weis, Nucl. Phys. B84 (1975) 141.
[12] S.D. Drell and T.-M. Yan, Phys. Rev. Letters 24 (1970) 181.
[13] N. Silvestrini, Proc. 16th Int. Conf. on high-energy physics, ed. J.D. Jackson and A. Roberts (NAL, Batavia, Ill., 1973) vol. 4, p. 1.
[14] D. Amati, R. Jengo, H.R. Rubinstein, G. Veneziano and M.A. Virasoro, Phys. Letters 27B (1968) 38;
D. Amati, L. Caneschi and R. Jengo, Nuovo Cimento 58A (1968) 783.
[15] J.H. Weis, Lawrence Radiation Laboratory report No UCRL-1978 (1970).
[16] P.N. Kirk et al., Phys. Rev. D8 (1973) 63.
[17] V.N. Gribov and L.N. Lipatov, Phys. Letters 37B (1971) 78; Yad. Fiz. 15 (1972) 781; Sov. J. Nucl. Phys. 15 (1972) 438;
G. Schierholz, Phys. Letters 47B (1973) 374.
[18] E.D. Bloom and F.J. Gilman, Phys. Rev. D4 (1971) 2901.
[19] J. Gayler, Daresbury Study Weekend (June 1971).
[20] A. Bodek et al., Stanford Linear Accelerator Center report No SLAC-PUB 1399 (1974).
[21] A. Bodek et al., Phys. Rev. Letters 30 (1973) 1087.
[22] S.J. Brodsky and G.R. Farrar, Phys. Rev. Letters 31 (1973) 1153.
[23] M. Hagenauer Proc. 17th Int. Conf. on high-energy physics, ed. J.R. Smith (Science Research Council, Chilton, Didcot, 1974) p. IV-95.
[24] V. Rittenberg and H.R. Rubinstein, Phys. Letters 35B (1971) 50.
[25] F. Brasse et al., Nucl. Phys. B39 (1972) 421.
[26] H.D. Dahmen and F. Steiner, Phys. Letters 43B (1973) 217.
[27] G. Schierholz, ref. [17].
[28] F.J. Gilman, 17th Int. Conf. on high-energy physics, ed. J.R. Smith, (Science Research Council, Chilton, Didcot, 1974) p. IV-149.
[29] M.G. Schmidt, Nuovo Cimento, to appear.